Title
DENSITY FLUCTUATIONS IN PREMIXED TURBULENT FLAMES

Authors
Namazian, M.
Talbot, L.
Robben, F.

Publication Date
1984-03-01

LBL-17666

Lawrence Berkeley Laboratory

UNIVERSITY OF CALIFORNIA

APPLIED SCIENCE DIVISION

To be presented at the 20th International Symposium on Combustion, Ann Arbor, MI, August 12-17, 1984

DENSITY FLUCTUATIONS IN PREMIXED TURBULENT FLAMES

M. Namazian, L. Talbot, and F. Robben

March 1984

APPLIED SCIENCE DIVISION

Prepared for the U.S. Department of Energy under Contract DE-AC03-76SF00098

Density Fluctuations in Premixed Turbulent Flames

M. Namazian, L. Talbot*

Mechanical Engineering Department
University of California,
Berkeley, CA 94720

and

F. Robben

Lawrence Berkeley Laboratory
University of California,
Berkeley, CA 94720

Mailing Address:

M. Namazian
Lawrence Berkeley Laboratory, B29C
University of California,
Berkeley, CA 94720

Subjects:

(1) Turbulent Combustion
(2) Structure of Combustion Wave
(3) Modeling

*Also Lawerence Berkeley Laboratory, University of California, Berkeley, CA 94720

ABSTRACT

The simultaneous two-point density fluctuations in a V-shaped turbulent flame are measured using a two-point Rayleigh scattering method. A wrinkle laminar flame model with finite instantaneous flame thickness is developed for the flames studied. The reaction front probability density function is both measured directly and also calculated from the measured mean density. An analytical expression for this pdf is given which is derived based on a thin flame model. The mean, rms and correlation coefficients are calculated using the finite reaction front thickness model and the results are compared with the experimental data. The pdf of the intermediate states are shown to be due to the reaction front thickness.

Introduction

The structure of turbulent flames is quite complex and not well understood in spite of numerous theoretical and experimental studies. In this paper the density fluctuations in relatively simple turbulent flames have been determined using the two-point Rayleigh scattering technique. A number of the characteristics are compared with the predictions of some simple modelling assumptions and shown to be in good agreement. This work is a continuation of previous studies on the velocity and density in this turbulent flame configuration (1,2), and in particular of the initial two-point Rayleigh scattering measurements (3).

Figure 1 shows a schematic diagram of the flame configuration and optics used for this study. The open jet nozzle for the premixed flow is 5 cm in diameter; the surrounding co-axial nozzle produces an air velocity the same as the mixture in the inner fuel jet and minimizes the inner jet boundary turbulence and its effect on the flame. The two-point density measurements reported in this paper were separated across the flame brush, the y direction. Further details of the combustor, optics and data collection system are given in Ref. (3).

Turbulence in the jet flow was generated either by a square grid, with 1 mm rods spaced 5 mm apart, or by a perforated plate with 3.2 mm holes and 4.8 mm spacing. Two different ethylene-air equivalence ratios were used to produce the flame conditions summarized in Table I. For each condition profiles in the y (transverse) direction were taken at four stations, 20 mm, 40 mm, 60 mm and 80 mm above the flame-holder. For each profile the separation of the two points was varied in about 8 steps from 0.0 to

10.0 mm in y direction. The mean, variance, correlation coefficient and probability density functions are reported in this paper.

Wrinkled Laminar Flame Model

For the conditions of these experiments the structure of the flame is described by the wrinkled laminar flame concept . This has been shown by the previously reported experimental measurements (3), further, the ratio of the turbulence intensity to the laminar flame speed, u'_∞ / S_u, is less than 1, placing these experiments in the wrinkled laminar flame regime (4,5). According to the wrinkled laminar flame model the turbulent flame brush consists of a thin laminar reaction front which fluctuates in shape and in location. Figure 2 shows the coordinate system used to describe the motion of the reaction front in one spatial dimension. The y axis is fixed in the laboratory frame with y=0 at the center of the turbulent flame brush. The ξ axis is attached to the instantaneous flame with ξ=0. being fixed at the center. The vertical axis is labeled by ρ for the density. On the same figure the mean density, $\bar{\rho}(y)$, and a schematic of the probability density function (pdf) of the position of the laminar flame, Q(y), are shown.

A similar approach in modelling the wrinkled laminar flame was previously employed by Smith and Gouldin (6). They assumed a triangular shape for the pdf of the reaction front. In this paper the pdf, Q(y), is calculated from the experimental data; further, the model is extended to two-point correlations and to the calculation of the pdf of the intermediate states.

An analytic expression for obtaining Q(y) from the mean turbulent flame profile can be found if a thin reaction front assumption is made, i.e., that the laminar flame thickness δ_f is much less than the turbulent flame brush thickness. In this case there are only burned or unburned states within the flame, and the probability of finding burned gas at point y will be given by

$$p_b(y) = \int_{-\infty}^{y} Q(y')dy' \quad (1)$$

In this equation Q(y)dy is the probability that the reaction front center will be found at y. The probability of finding unburned gas at point y is the complementary expression given by:

$$p_u(y) = 1-p_b(y) = \int_y^{\infty} Q(y')dy' \tag{2}$$

The mean density at point y is then given by

$$\bar{\rho}(y) = \rho_u p_u(y) + \rho_b p_b(y) = \rho_u - (\rho_u - \rho_b)\int_{-\infty}^{y} Q(y) \tag{3}$$

By differentiating equation (3) with respect to y, Q(y) may be found:

$$Q(y) = -\frac{1}{1-\frac{\rho_b}{\rho_u}} \cdot \frac{d}{dy}\left(\frac{\bar{\rho}(y)}{\rho_u}\right) \tag{4}$$

Using Eq. (4) Q(y), the probability that the flame center is located at y, can be found from the measured $\bar{\rho}$ (y). The validity of the thin reaction front approximation is discussed later. If a finite thickness fluctuating flame front is assumed, a simple algorithm for Q(y) cannot be obtained and it would be necessary to use a more complex procedure, such as a curve fitting, successive approximation algorithm.

Expressions for the mean, variance, covariance, and probability density function based on a finite thickness instantaneous flame front, with profile $\rho_f(\xi)$, will now be developed. Referring to Fig. 2, the origin of the ξ coordinate is fixed at the center of the fluctuating instantaneous flame. Thus Q(y)dy is the differential probability for the origin of the ξ coordinate, to be at location y. It can then be seen that the differential probability that $\xi=\xi_1$, is at the location y is just*

$$p(\xi_1)dy = Q(y-\xi_1)dy$$

---

* $prob\,[y-\frac{dy}{2}<\xi=\xi_1<y+\frac{dy}{2}]=prob\,[y-\xi_1-\frac{dy}{2}<\xi=0<y-\xi_1+\frac{dy}{2}]=Q(y-\xi_1)dy$

Similarly, the differential probability that $y = y_1$ is at the location ξ is**

$$p(y_1)d\xi = Q(y_1 - \xi)d\xi$$

The mean density, for instance, is then given by

$$\bar{\rho}(y) = \int \rho_f(\xi)\, p(y) d\xi$$
$$= \int \rho_f(\xi)\, Q(y-\xi) d\xi$$

The instantaneous flame profile $\rho_f(\xi)$ is assumed to be the same as the laminar flame profile and is obtained directly by Rayleigh scattering measurements of a laminar flame at the same equivalence ratio. This is accomplished using the same apparatus with the turbulence generating grid removed, with the measurement performed close to the flame-holder. This profile differs from the asymptotic values of ρ_u and ρ_b only over the distance δ_f about the flame center. Let us define

$$\rho_f(\xi) = \rho_b \quad \text{for } \xi > \frac{\delta_f}{2}$$
$$= \rho_l(\xi) \quad \text{for } -\frac{\delta_f}{2} < \xi < \frac{\delta_f}{2}$$
$$= \rho_u \quad \text{for } \xi < -\frac{\delta_f}{2}$$

The mean and variance are then given by

$$\bar{\rho}(y) = \int_{-\infty}^{\infty} \rho_f(\xi) Q(y-\xi) d\xi \tag{5}$$

$$\overline{\rho'^2}(y) = \int_{-\infty}^{\infty} \rho_f^2(\xi)\, Q(y-\xi) d\xi - \bar{\rho}^2(y) \tag{6}$$

When density measurements are taken simultaneously at two different y positions, separated by δ, the covariance can be defined as

$$cov(\rho_1, \rho_2) = \frac{1}{T}\int_0^T \rho_1(t)\rho_2(t) dt$$

**Note dy=d ξ and

$$prob\,[\xi + \frac{d\xi}{2} > y_1 > \xi - \frac{d\xi}{2}] = prob\,[y_1 - \frac{dy}{2} < \xi < y_1 + \frac{dy}{2}] = Q(y_1 - \xi)dy = Q(y_1 - \xi)d\xi$$

This equation simply means that the motion of a differential y_1 seen by an observer standing at ξ is the same as the motion of a differential element ξ to an observer standing at y_1.

in terms of the time dependent variables ρ_1 (t) and ρ_2 (t). Using the flame model of Fig. 2 and the probability of the instantaneous flame location Q(y), the covariance of the density is given by***

$$cov(y,y+\delta) = \int_{-\infty}^{\infty} \rho_f(\xi)\rho_f(\xi+\delta)Q(y-\xi)d\xi - \bar{\rho}(y)\bar{\rho}(y+\delta). \tag{7}$$

The correlation coefficient of density fluctuations is then given by

$$R(y,\delta) = \frac{cov(y,y+\delta)}{(\overline{\rho'^2}(y)\overline{\rho'^2}(y+\delta))^{1/2}} \tag{8}$$

To find the pdf of the density fluctuations at a given point y we convert the probability domain from ξ to $\rho=\rho_f(\xi)$,where $\rho_f(\xi)$ represents the laminar flame density profile. It was stated above that the probability of y_1 falling in a differential region of the laminar flame at ξ is $Q(y_1-\xi)d\xi$. Let us define $q_{y_1}(\rho)d\rho$ to be the probability of y_1 falling in a differential region of the laminar flame with density ρ. These two probabilities are identical, ie $q_{y_1}(\rho)d\rho=Q(y_1-\xi)d\xi$, which gives:

$$q_{y_1}(\rho) = \frac{Q(y_1-\xi)}{\frac{d\rho_f(\xi)}{d\xi}} \tag{9}$$

In this equation for the pdf of the density both ξ and $d\rho_f(\xi)/d\xi$ are evaluated from $\rho_f(\xi)$ at the value ρ.

It is obvious that $q_{y_1}(\rho)$, the pdf of the density at point y_1 , will have an infinite value when ρ_f assumes the unburned and burned values, ρ_u and ρ_b, where $d\rho_f(\xi)/d\xi=0$. This represents two delta functions corresponding to unburned and burned densities, ρ_u and ρ_b. For $\rho_u>\rho>\rho_b$, $d\rho_f(\xi)/d\xi$ is non-zero and thus q_{y_1} will have

---

***For the case that $\delta\geq\delta_f$ (δ is distance between sampled points)

$$COV(y,y+\delta)= \int_{-\infty}^{-\delta-\delta_f/2} \rho_u^2 Q(y-\xi)d\xi + \int_{-\delta-\delta_f/2}^{-\delta+\delta_f/2} \rho_\xi\rho_u Q(y-\xi)d\xi + \int_{-\delta+\delta_f/2}^{-\delta_f/2} \rho_u\rho_b Q(y-\xi)d\xi$$

$$+ \int_{-\delta+\delta_f/2}^{-\delta_f/2} \rho_u\rho_b Q(y-\xi)d\xi + \int_{-\delta_f/2}^{+\delta_f/2} \rho_b\rho_\xi Q(y-\xi)d\xi$$

$$+ \int_{\delta_f/2}^{+\infty} \rho_b^2 Q(y-\xi)d\xi - \bar{\rho}(y)\bar{\rho}(y+\delta)$$

The covariance equation for two other cases of $\frac{\delta_f}{2}<\delta<\delta_f$ and $0.=<\delta<\frac{\delta_f}{2}$ also could also be defined similarly.

a finite, non-zero value in this range which represents the intermediate states of density.

Experimental data and comparison with model predictions

In Fig 3 the mean flame density profile $\bar{\rho}(y)$ and the pdf of the reaction front Q(y) as calculated from Eq.(4), are shown. A two-point Rayleigh method was also used to directly measure Q(y) and is shown by the circles and the dashed line through them. There is good agreement with the result derived from Eq.(4). The directly measured Q(y) was determined by measuring the fraction of the time that the front was found between the two measurement points, as a function of the location of two measurement points across the flame brush. The separation between the sampling points was 1.2 mm while the laminar flame thickness was about 1.0 mm. Similar results were obtained for other stations and the other flame conditions listed in Table I.

Figure 4 shows the experimental measurements and model predictions for the normalized mean density and the normalized rms density fluctuations at the same locations as in Fig. 3. The lines represent the model predictions based on Eqs. (5) and (6) and the points are the experimental data.

In Fig. 3 good agreement is obtained between the two methods for determining Q(y). The thin instantaneous flame approximation made in deriving Eq.(4) should be quite good for the thick flame of Fig. 3b, but may result in some error for the conditions of Fig. 3a, where the turbulent flame has a thickness of about 3mm and the laminar flame thickness is about 1mm. The approximation used in Eq.(4) will result in lower maximum value for Q(y); in Fig. 3a the calculated value is about 10% smaller. In Fig. 4 excellent agreement is found between the experimental results and the modeling predictions of the mean density. These predictions are based on Eq.(5) and includes the laminar flame thickness, supporting the accuracy of the thin instantaneous flame approximation used for obtaining Q(y).

The agreement between the experiment and model predictions for the rms density fluctuations are also good for the thicker flame of Fig. 4b., but the model predictions are somewhat larger for the thinner flame of Fig. 4a. At the center of the flame brush the model predicts rms values of 0.35 and 0.40 for Fig. 4a and Fig. 4b respectively; the corresponding experimental values are 0.30 and 0.40. In this model, therefore, the rms fluctuation is a function of the flame thickness and thus the height above the flame-holder. In the thin flame approximation, as shown by Liby and Bray (7), the rms density fluctuations are a function of unburned, burned and local densities. The maximum at the center of the brush is a function of burned and unburned densities only and for both cases of Fig. 4a and Fig. 4b the predicted rms fluctuations by the thin flame model are 0.42 as compared to the experimental values of .30 and 0.40.

Good agreement with the model predictions from Eq.(8) is obtained for the two-point correlation coefficient, as shown in Fig. 5. The data are plotted as a function of distance δ between the two sample points, with the one of the points always kept at the center of the turbulent flame. Data for three axial locations, and for the three different flame conditions, are shown. For the 20mm axial location the measured correlation is a bit larger than the model predictions. This is consistent with the lower rms fluctuation at the same location, shown in Fig. 4a.

For all the cases studied the correlation coefficient and therefore the length scale associated with the density fluctuations increases with the distance above the flame-holder. For a given height above the flame-holder the correlation coefficient is least for the flame 1 and is largest for flame 2(Table I).

The experimental and predicted values of the density pdf are shown in Fig. 6 for different locations in the flame brush with an axial location of 40mm, and in Fig. 7 for the center of the flame brush at different axial locations. The experimental measurements include photomultiplier noise, and thus are somewhat different from the model predictions of Eq.(9) for the density without noise. For the rms fluctuations shown in Fig. 4 the photomultiplier noise was subtracted out(2,3), however, there is no simple way to remove this noise from the pdf.

As mentioned previously, the model properly predicts a singular value of the pdf at ρ_u and ρ_b , and thus the model curve asymptotically approaches infinity at these densities. For the experimental data the phtomultiplier noise broadens these singularities and leads to peaks of finite height and width. In these end regions of the pdf the photomultiplier noise dominants the experimental data and the measured results cannot be compared with the model. However, the effect of the noise is to broaden any peak and thus will have little effect for intermediates values where the pdf is rather flat.

In all cases the model predictions are in relatively good agreement with the measured intermediate state densities. In particular, the decrease in the intermediate states with distance from the flame-holder predicted by the model is in agreement with the experimental measurements. This decrease in the intermediate states at distances further away from the flame-holder is due to the increase in the flame brush thickness, and thus the ratio with the laminar flame thickness, which decreases the probability that the measurement point will fall within the laminar flame region. It is clear that the finite instantaneous flame thickness is responsible for the intermediate state density. In these experiments both the spatial resolution and the time response of the measurement technique were adequate to ensure at most a small correction.

The experimental intermediate state densities are consistently somewhat larger than the predictions. For the 20.mm axial location the lower predictions could be due to the thin reaction front assumption used in calculating Q(y). For the larger axial locations the thin reaction front assumption is reasonable and there should be little error in Q(y). However, there is another mechanism which would broaden the effective laminar flame and may be responsible for the larger measured intermediate states. High speed movies of the flame surface show an increase in the convolutions and angular orientations of the flame at larger distances from the flame-holder(8). These convolutions would cause the flame to cross the measurement point at steep angles and thus increase the effective instantaneous flame thickness.

Conclusions

The density fluctuations in a turbulent V-shaped flame were measured using a two-point Rayleigh scattering technique. A wrinkled laminar flame model of the flame is developed. The probability density function of the reaction front used in this model is both measured and calculated. The calculated mean density profile is always in good agreement with the experimental data. Both the measured and calculated rms fluctuations increase with the height above the flame-holder. The predicted rms is a bit too large for locations close to the flame-holder

The correlation coefficient between the density fluctuations increases with the height above the flame-holder. The model also predicts the same trend with good agreement between the experimental and predicted values.

The intermediate states are due to the laminar flame thickness. The predicted values for the intermediate states are smaller than the measurements. The intermediate states are relatively large at locations close to the flame-holder.

Acknowledgement

This work was supported by Air Force Office of Scientific Research under Contract F-44620-76-C-0083. Additional equipment and facility support was provided by the Chemical Sciences Division of the U.S. Department of Energy under contract DE-AC-03-76SF00098.

References

1. Bill, R. G., Jr., Namer, I., Talbot, L., Cheng, R. K., and Robben, F.: *Combustion and Flame, 43* ,No. 3, pp 229 (1981).

2. Bill, R. G., Jr., Namer, I., Talbot, L. and Robben, F.: *Combustion and Flame, 44* , 277-285 (1982).

3. Namazian, M., Talbot, L., Robben, F., and Cheng, R. K.: *Nineteenth Symposium (Int'l) on Combustion* ,p. 487, The Combustion Institute (1983).

4. Andrews, G. E., Bradley, D. and Lwakabamba, B.: *Combustion and Flame, 24* ,285-304 (1975)

5. Ballal, D. R. and Lefebvre, A. H.: *R. Soc. Lond. A. 344* ,217-234 (1975)

6. Smith K., O. and Gouldin, F., C.: *AIAA Journal* Vol. 17, No. 11 Nov.(1979)

7. Libby, P. and Bray, K., N., C.: *AIAA J.* 15:1186 (1977)

8. Hertzberg, J. R., Namazian, M. and Talbot, L. to appear in *Combustion Science and Technology* (1984).

TABLE I Experimental Conditions

No.	Equiv. ratio	U_∞ (m/s)	turb. source	$(u'/U)_\infty$ (%)
1	0.6	7.0	grid	5.0
2	0.6	7.0	plate	7.0
3	0.8	7.0	grid	5.0

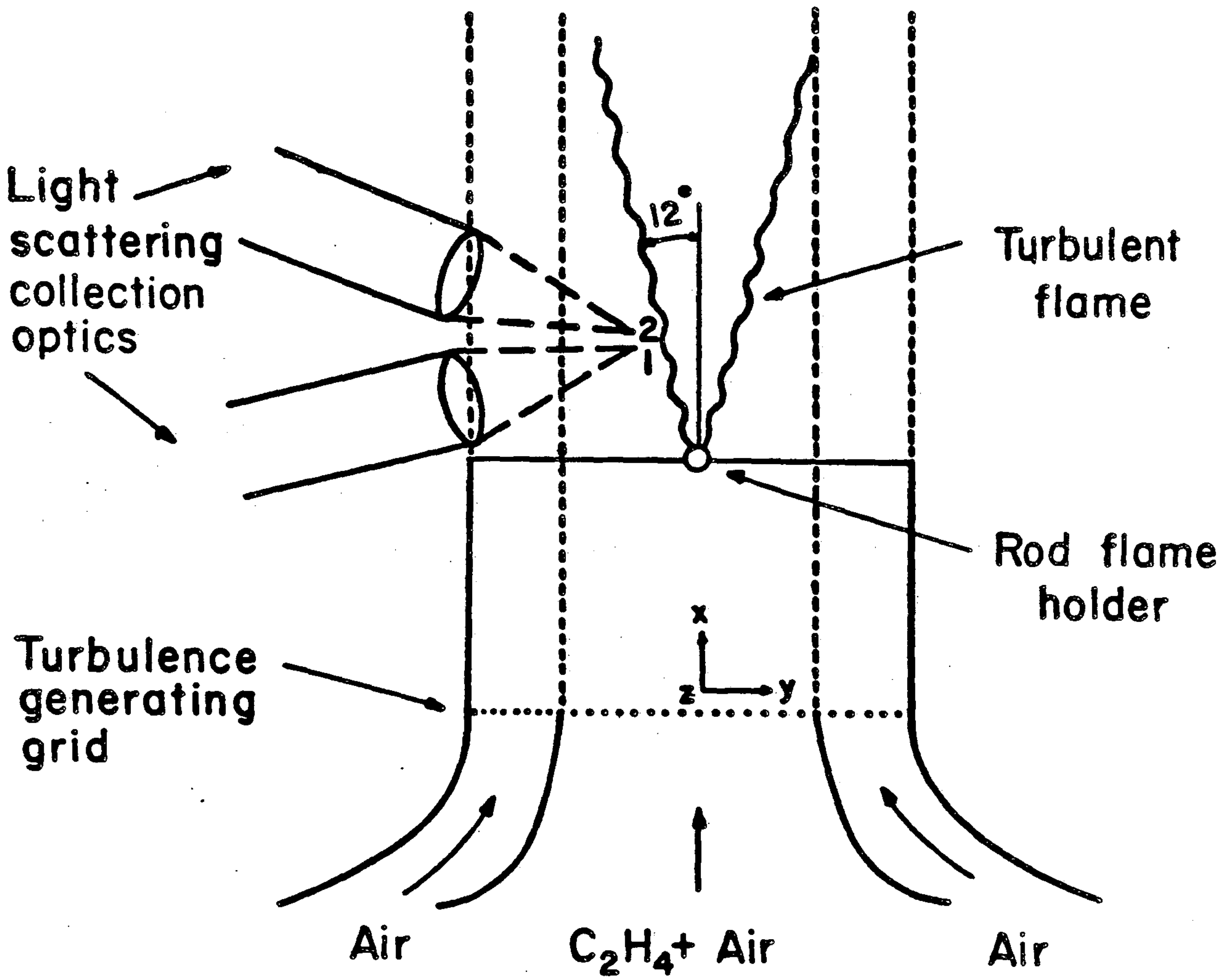

XBL 823-8761

Fig. 1 Schematics of the experimental apparatus for two-point Rayleigh scattering measurement.

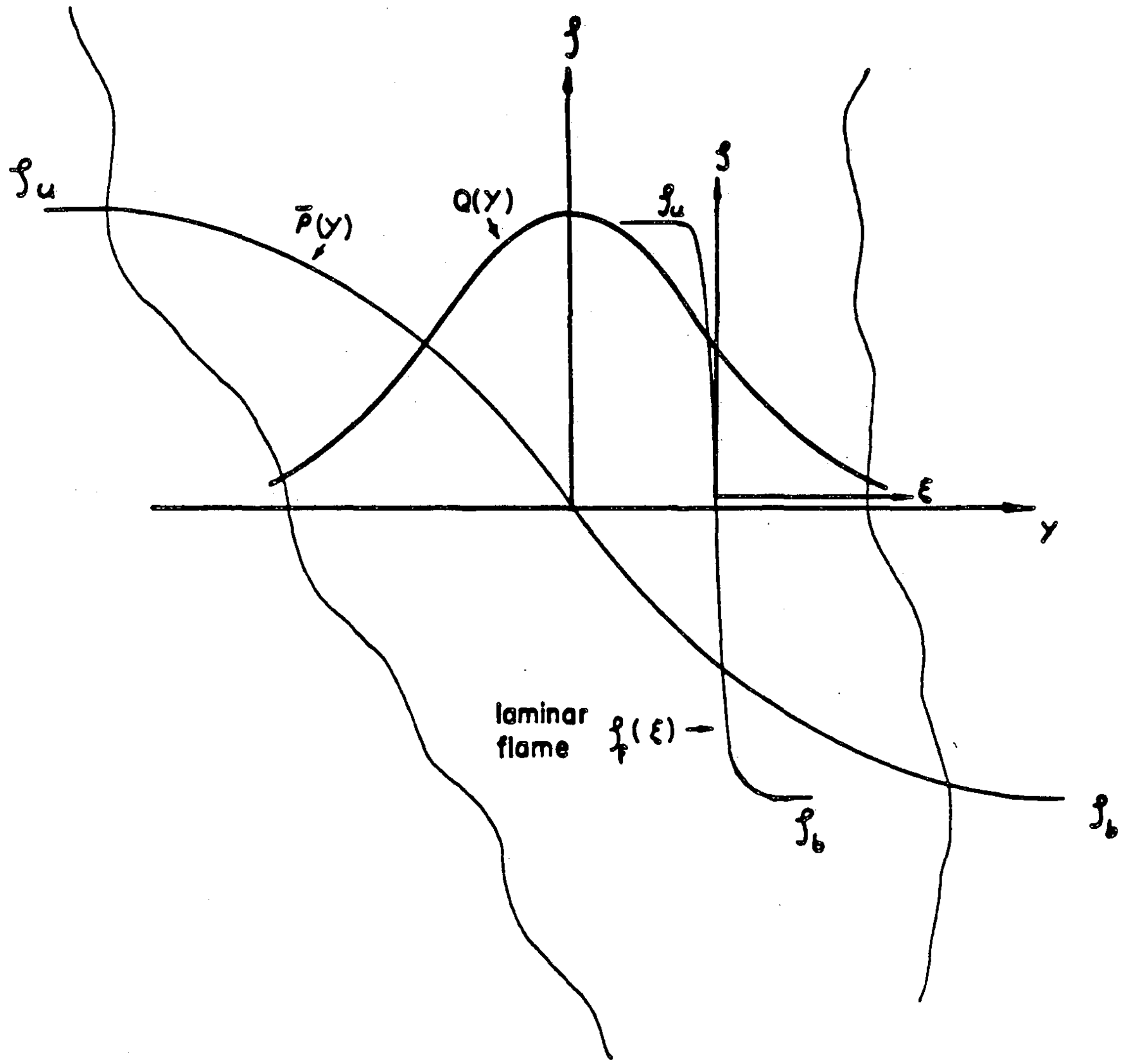

XBL 841-375

Fig. 2 Coordinate system of the wrinkled laminar flame model with moving ξ axis attached to the center of the laminar reaction front and the stationary y axis fixed to the center of the turbulent flame brush.

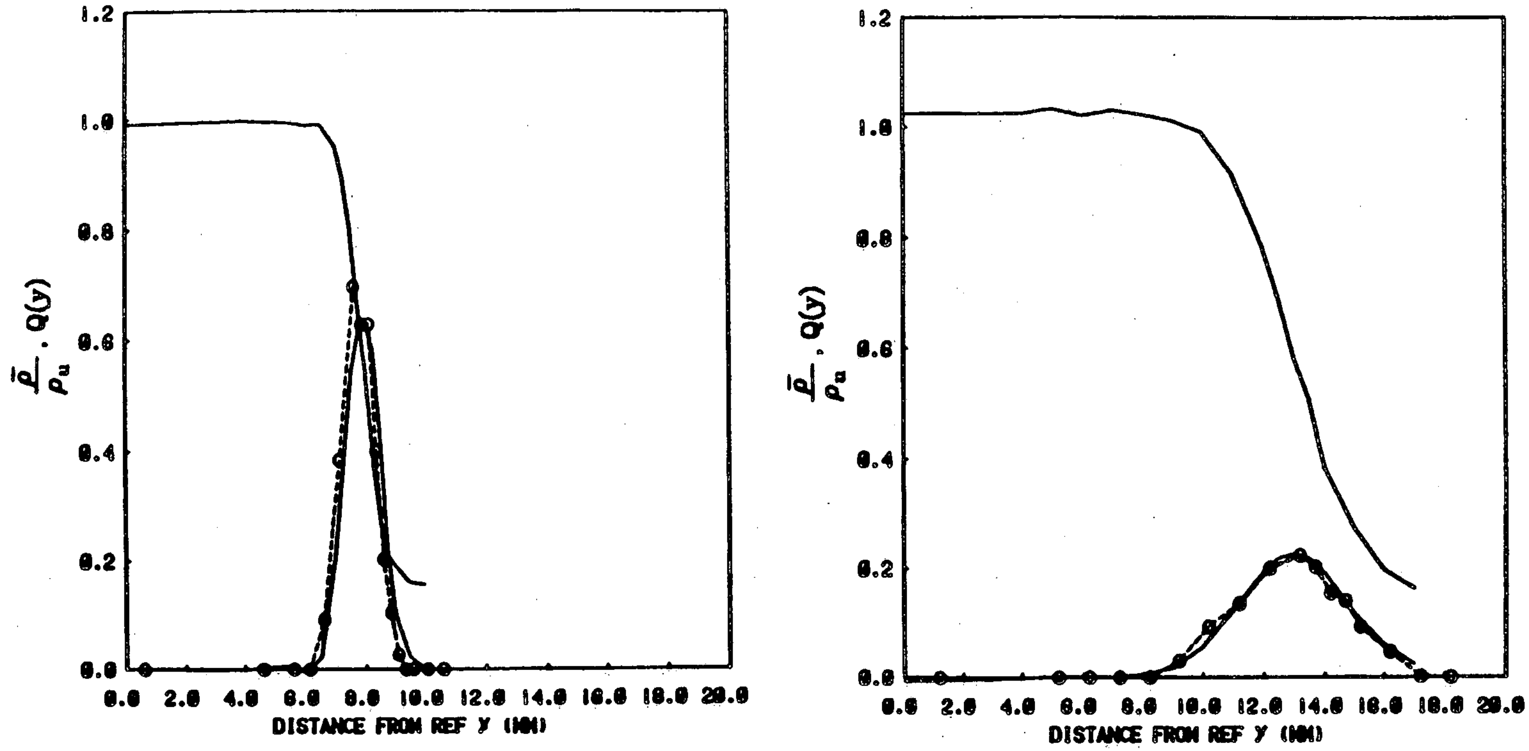

(a) (b)

XBL 841-376

Fig. 3a,b Measured mean density profile and measured(solid line) and calculated(points and dashed line) pdf of the reaction front position inside the flame brush for flame No.(1) at 20mm(a) and 80mm(b) above the flame holder.

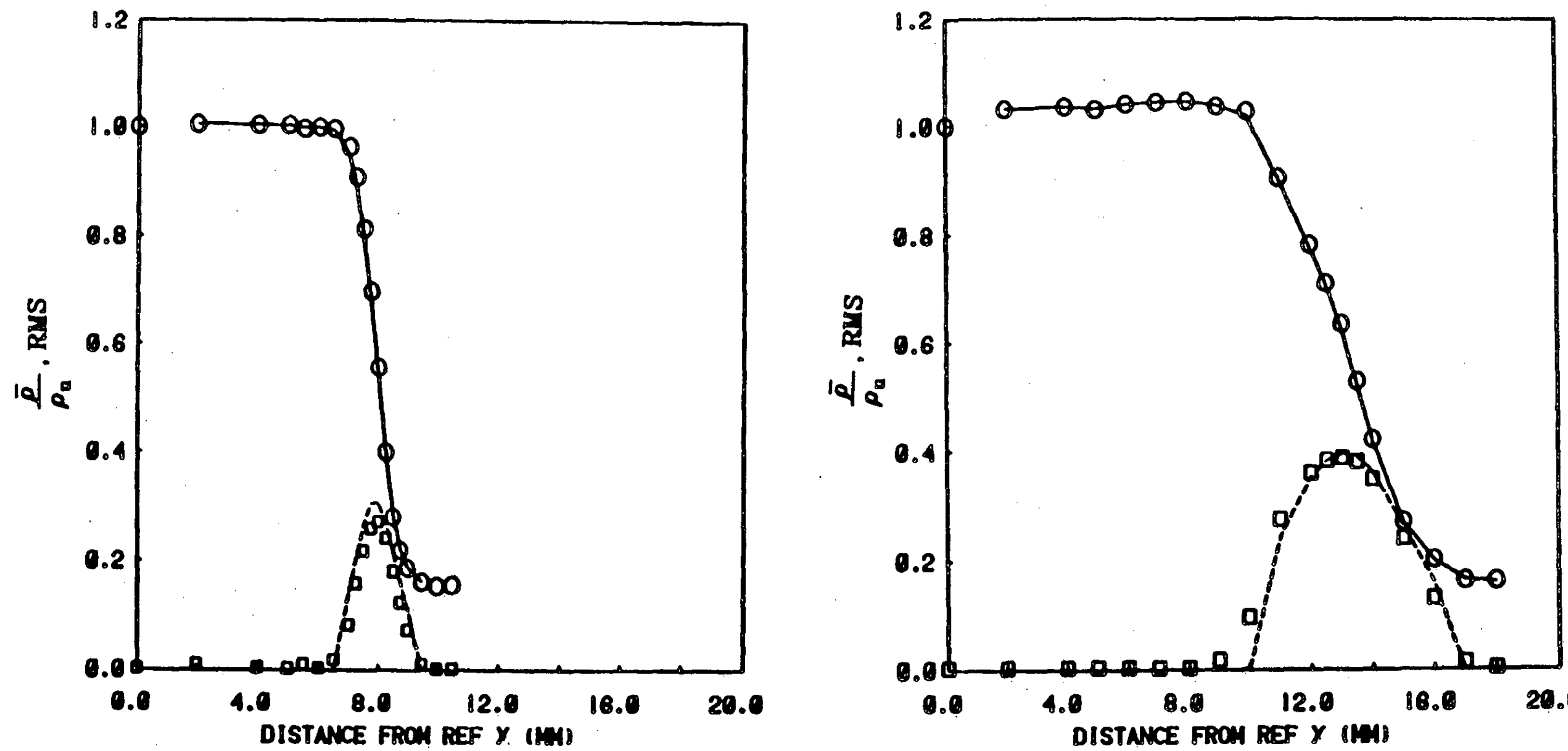

(a) (b)

XBL 841-377

Fig. 4a,b Measured(points) and calculated(lines) mean density profile and rms density fluctuations for flame No.(1) at 20mm(a) and 80mm(b) above the flame holder.

(a)

(b)

(c)

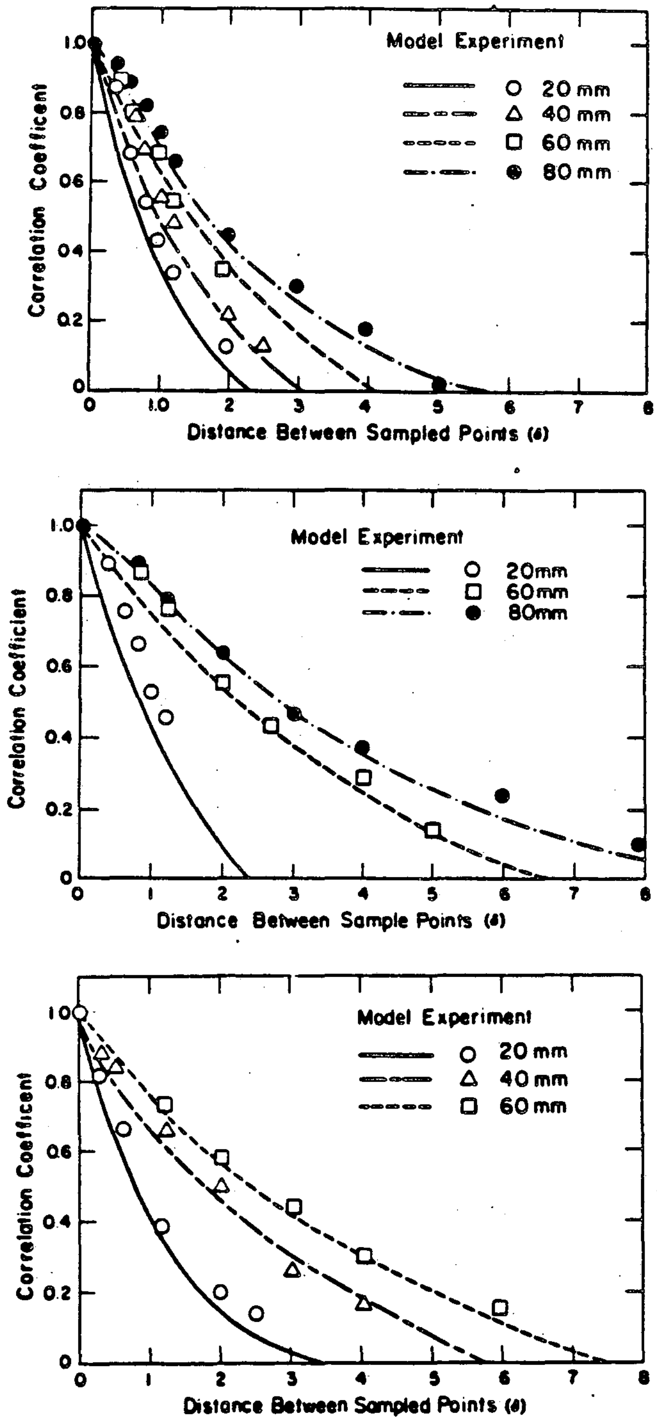

XBL 841-378

Fig. 5a,b,c Measured and calculated correlation coefficient of the density fluctuations at two points separated by δ, with one of the points fixed at the center of the flame brush, plotted against δ for flame No. 1(a), No. 2(b) and No. 3(c).

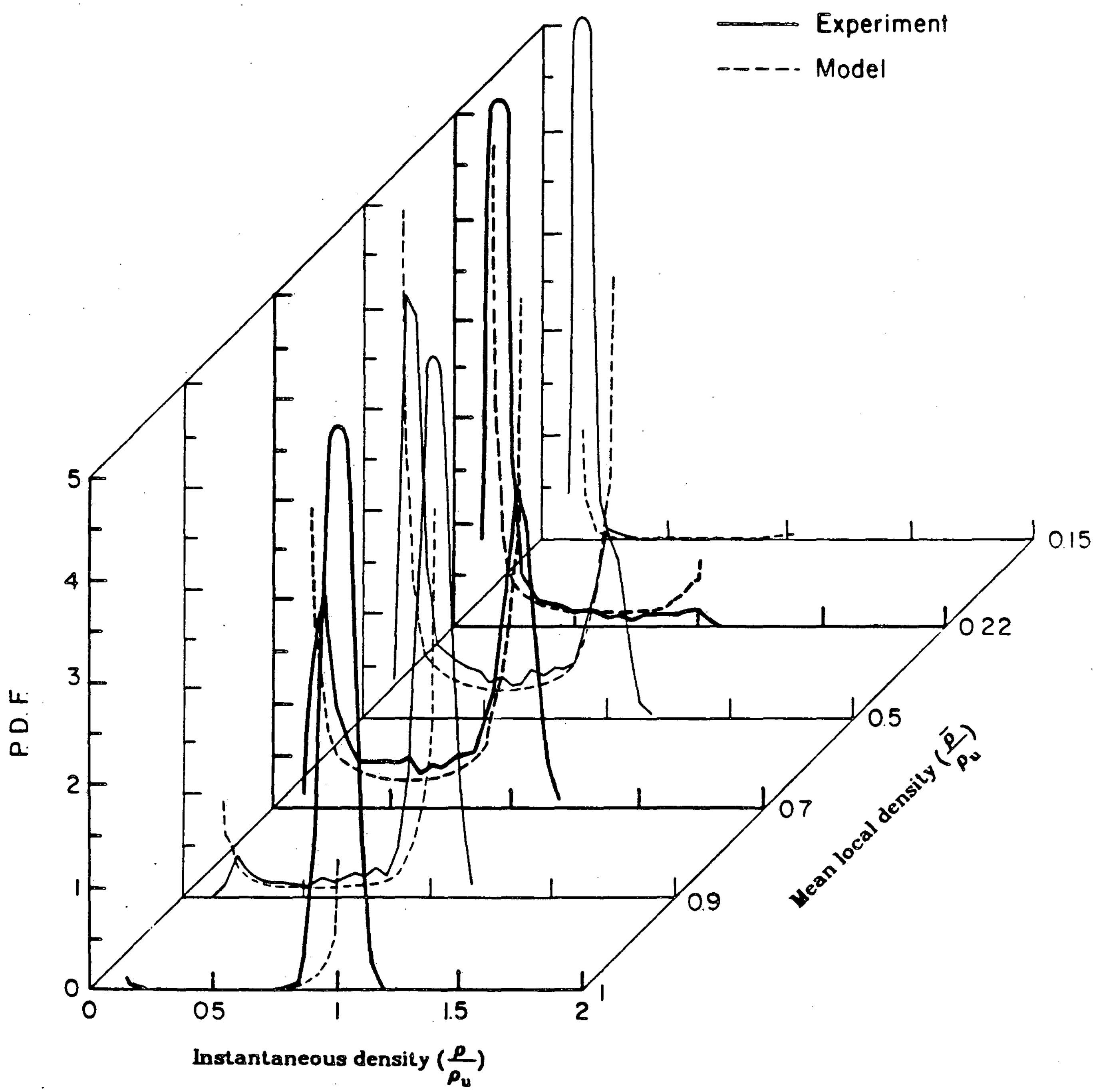

XBL 841-379

Fig. 6 Measured and calculated density pdf for different locations in the flame brush at axial location of 40.mm in flame No.(1). The horizontal axis of this figure represents the instantaneous density and the oblique axis represents the mean density at measurement points.

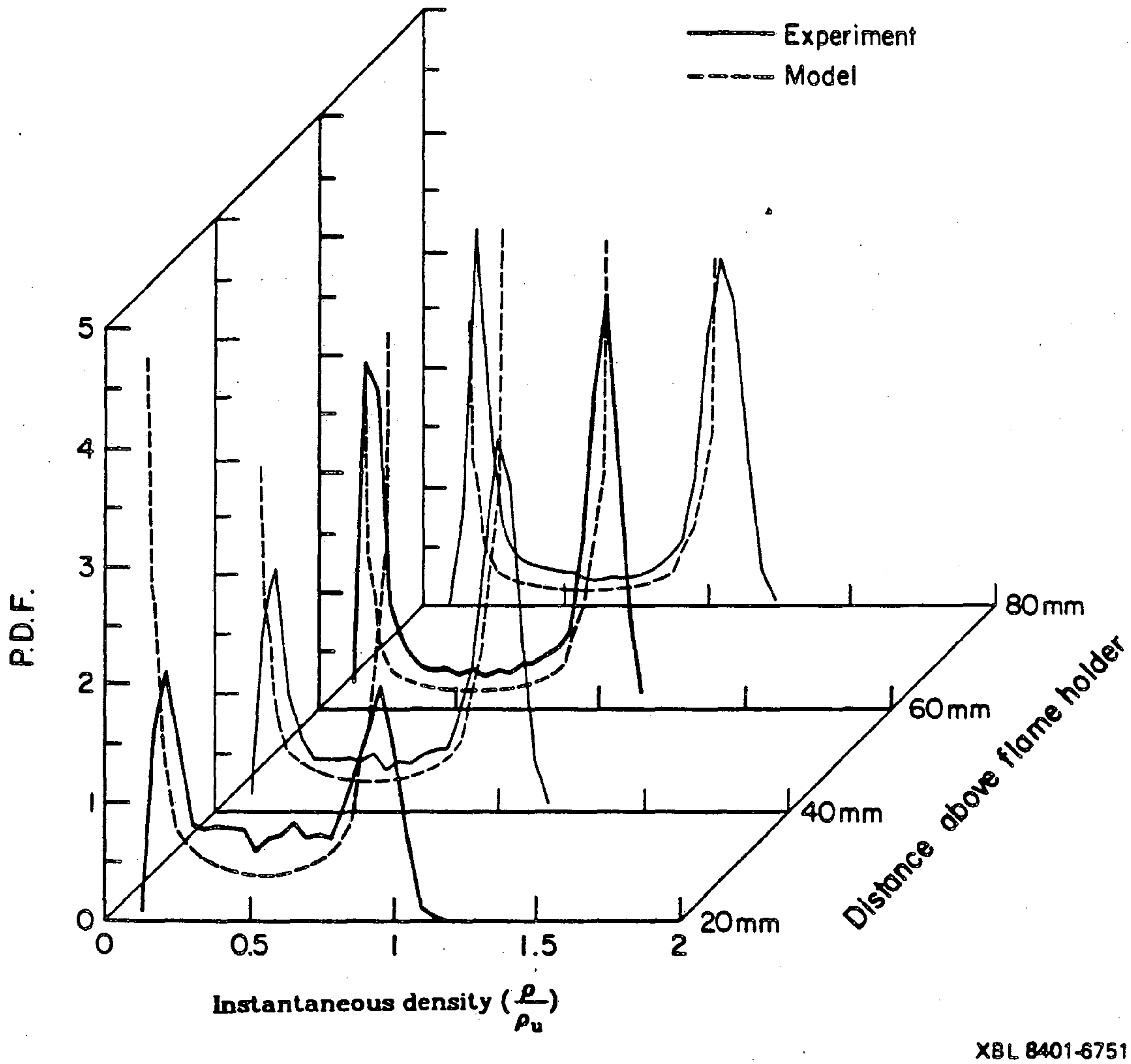

Fig. 7 Measured and calculated density pdf for the center of flame No. 1 at different axial locations above the flame holder.

TECHNICAL INFORMATION DEPARTMENT
LAWRENCE BERKELEY LABORATORY
UNIVERSITY OF CALIFORNIA
BERKELEY, CALIFORNIA 94720